Computational Predictive and Electrochemical Detection of Metabolites (CP-EDM) of Piperine

Asra, Ridho; Povinelli, Ana Paula Ribeiro; Zazeri, Gabriel; Jones, Alan M

DOI:
10.26434/chemrxiv-2024-4lt9w

Document Version
Other version

Citation for published version (Harvard):
Asra, R, Povinelli, APR, Zazeri, G & Jones, AM 2024 'Computational Predictive and Electrochemical Detection of Metabolites (CP-EDM) of Piperine' ChemRxiv. https://doi.org/10.26434/chemrxiv-2024-4lt9w

Computational Predictive and Electrochemical Detection of Metabolites (CP-EDM) of Piperine

Ridho Asra[1], Ana P.R. Povinelli[2], Gabriel Zazeri[3],* and Alan M. Jones[1]*

[1] School of Pharmacy, College of Medical and Dental Sciences, University of Birmingham, Edgbaston, B15 2TT, UK

[2] Departament of Physics, Instituto de Biociências, Letras e Ciências Exatas (IBILCE), UNESP, Rua Cristovão Colombo 2265, São José do Rio Preto CEP 15054-000, SP, Brazil;

[3] Departament of Physics, Universidade Federal de Roraima (UFRR). Av. Cap. Ene Garcês, 2413 - Aeroporto, Boa Vista, 69310-000, RR, Brazil;

Correspondence: G.Z. gabriel.zazeri@ufrr.br , A.M.J. a.m.jones.2@bham.ac.uk

Keywords

Piperine, Metabolite, Electrochemical, Detection, Predictive, CP-EDM

Graphical Abstract

Abstract

In this article we introduce a proof of concept strategy: Computational Predictive and Electrochemical Detection of Metabolites (CP-EDM) to expedite the discovery of drug metabolites. The use of a bioactive natural product, piperine, that has a well curated metabolite profile but has an unpredictable computational metabolism (Biotransformer v3.0) was selected. We developed an electrochemical reaction to oxidise piperine into a range of metabolites, which were detected by LC-MS. In turn, a series of chemically plausible metabolites were predicted based on ion-fragmentation patterns. These metabolites were docked into the active site of CYP3A4 using Autodock4.2 From the clustered low-energy profile of piperine in the active site it can be inferred that the most likely metabolic position of piperine (based on intermolecular distances to the Fe-oxo active site) is the benzo[*d*][1,3]dioxole motif. The metabolic profile was confirmed by literature comparison and the electrochemical reaction delivered plausible metabolites *vide infra*. Thus, demonstrating the power of the hyphenated technique of tandem electrochemical detection and computational evaluation of binding poses. Taken together, we outline a novel approach where diverse data sources are combined to predict and confirm a metabolic outcome for a bioactive structure.

Introduction

An understanding of the major circulating metabolites that are generated from a parent biologically active molecule is of critical importance in drug discovery campaigns.[1] One powerful and emerging approach to detect and identify drug metabolites is the use of electrochemical techniques.[2-15] An alternative approach is to computationally predict via docking how a drug might interact with a cytochrome. [16-18] However, approaches that interlink these two complementary techniques are not delineated at present.

We have a long-standing interest in the chemistry [19] and molecular interactions [20] of the biologically active natural product, piperine. Piperine is a potent inhibitor of cytochrome CYP4A6 and related familial isoforms [21-22] but to the best of our knowledge the exact biological mechanism by which piperine is metabolised remains unknown.[23] There is, however, a body of evidence of typical piperine metabolites to enable confirmation by comparison. [24-27]

Results and Discussion

Prior to electrochemical reaction the cyclic voltammetry behaviour of piperine was measured [28] We have previously shown the voltammetric behaviour of a drug molecule is inversely correlated to it *in situ* metabolic half-life.[29] Using ferrocene (Fc/Fc^{+}) as an internal standard for the *pseudo* Ag/AgCl wire reference electrode and a glassy carbon electrode (GCE) as the working electrode and a platinum wire as the counter electrode (CE), the cyclic voltammetry behaviour of piperine was explored (**Figures 1 a-c**).

a

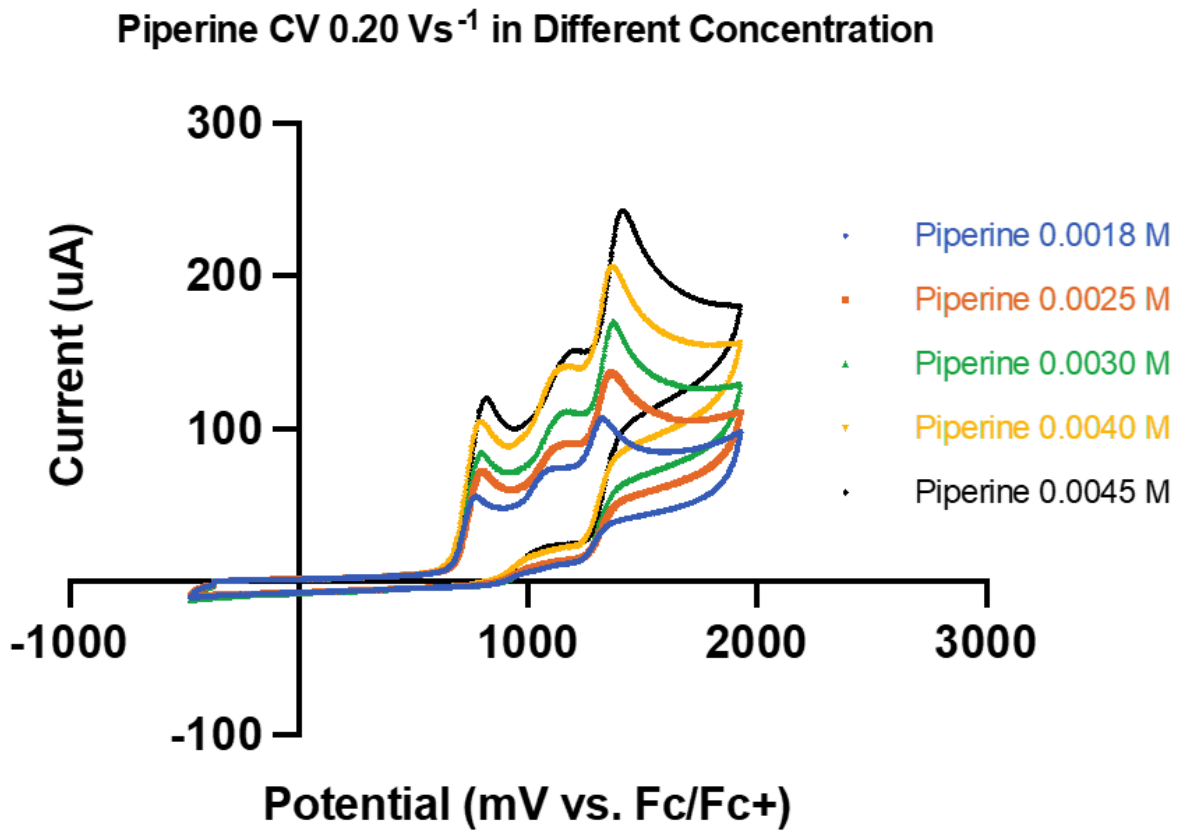

b

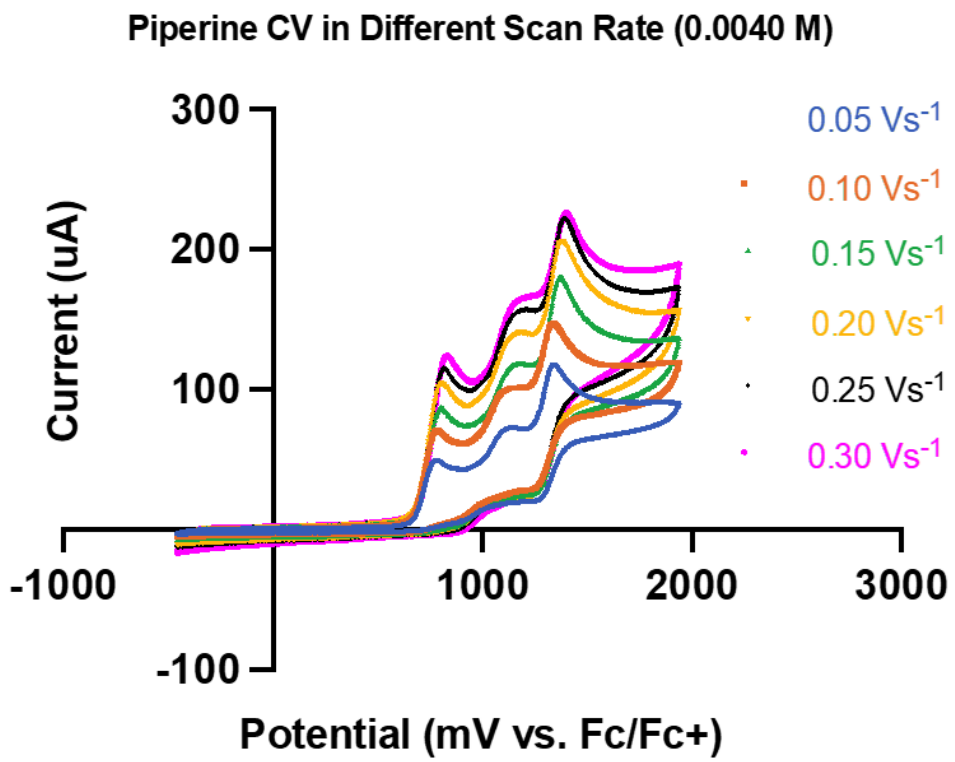

c

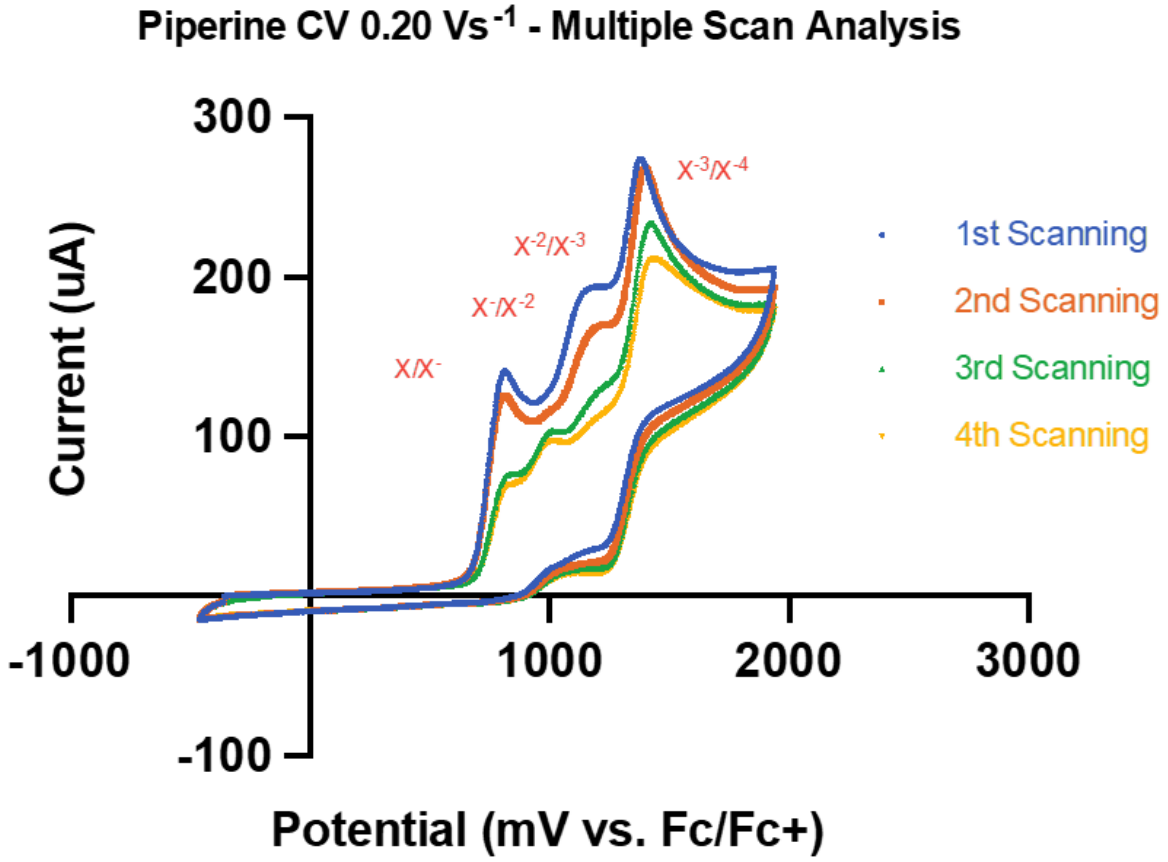

Figure 1. Cyclic voltammetry behaviour of piperine (concentrations varied), GCE (WE), Pt (CE), Ag/AgCl (pseudo RE) standardised to Fc/Fc^{+}. Electrolyte: $TBAPF_6$; solvent: MeCN. **a)** effects of piperine concentration on cyclic voltammetry behaviour - *Conditions:* start potential = 0 V_{reff}; upper vertex potential = 2.30 V_{reff}; lower vertex potential = -0.10 V_{reff}; stop potential = 0 V_{reff}; number of scans

= 1; υ: 0.20 Vs^{-1}; Step: 0.00244 V. [Piperine (0.0018 M: E_p = 0.745 V; i_p = 58 μA); piperine (0.0025 M: Ep = 0.766 V; ip = 75 μA); piperine (0.0030 M: E_p = 0.789 V; i_p = 84 μA); piperine (0.0040 M: E_p = 0.779 V; i_p = 103 μA); and piperine (0.0045 M: E_p = 0.805 V; i_p = 118 μA)]. **b)** effects of υ on piperine cyclic voltammetry behaviour- *Conditions:* start potential = 0 V_{reff}; upper vertex potential = 2.30 V_{reff}; lower vertex potential = -0.10 V_{reff}; stop potential = 0 V_{reff}; number of scans = 1; υ: 0.05-0.30 Vs^{-1}; step = 0.00244 V. [υ = 0.05 Vs^{-1}: E_p = 0.740 V; i_p =50 μA; υ = 0.10 Vs^{-1}: E_p =0.759 V; i_p = 72 μA; υ = 0.15 Vs^{-1}: E_p = 0.771 V; i_p = 87 μA; υ = 0.20 Vs^{-1}: E_p 0.788 V; i_p 105 μA; υ = 0.25 Vs^{-1}: E_p = 0.801 V; i_p = 115 μA; υ = 0.30 Vs^{-1}: E_p = 0.818 V; i_p = 123 μA]. **c)** effects of multiple scanning on piperine cyclic voltammetry behaviour – *Conditions:* start potential = 0 V_{reff}; upper vertex potential = 2.30 V_{reff}; lower vertex potential = -0.10 V_{reff}; stop potential = 0 V_{reff}; number of scans = 4; υ = 0.25 Vs^{-1}; step = 0.00244 V. *Scan 1:* E_p = 0.828 V; i_p = 139 μA. *Scan 2:* E_p = 0.801 V; i_p = 125 μA. *Scan 3:* E_p = 0.840 V; i_p = 76 μA. *Scan 4:* E_p = 0.850 V; i_p = 70 μA.

Figure 1a shows that the peak current (i_p) of piperine increases with increasing analyte concentration because there are more redox-active species available to undergo oxidation at the electrode surface, and with increasing the scan rate (**Figure 1b**), the electrode potential changes more rapidly, and the rate of electron transfer reactions increases, leading to a larger peak current. These are consistent with the Randles-Sevcik equation and indicate the diffusion-controlled redox process. In this Randles-Sevcik equation at 25 °C [30], (i_p= k $n^{3/2}$ A $\sqrt{Dv}$ C), i_p is the peak current, k is a constant of 2.69 x 10^5 C/ mol$\sqrt{v}$, n is the number of electrons, A is the electrode area (cm^2), D is the analytes diffusion coefficient (cm^2/s), v is the rate at which the potential is swept (V/s), and C is concentration. The peak potential (Ep) depends on the scan rate or concentration if the oxidation peak potential shifts to more positive potentials, and the non-scan rate is dependent if the E_p remains relatively constant as the scan rate and concentration increase. This study showed that piperine's electrochemical reaction is not concentration-dependent (range concentration 0.0025-0.0040 M). However, the E_p slightly changed to a more positive potential at C = 0.0045 M, which means the reaction becomes unstable at higher concentrations. In the differential scan rate analyses (**Figure 1b**), it showed that the reaction slightly changed and was not significant. Proving that changing the scan rate does not affect the electrochemical reactions. Changing to the multiple scanning of potential waveforms provides several pieces of information, including reversibility or irreversibility of an electrochemical reaction. **Figure 1c** depicts the multiple features of piperine CVs when using different applied potentials, and the apparent reversibility of some oxidation waves depends on the reversibility of later oxidation waves. Specifically, if the oxidation process generates an unstable species that degrades, all subsequent processes will be affected. For example, when scanning positively with applied potential, piperine will have four oxidation events with two return-reduction waves observed. For the next scanning, the reduction of X/X^- means the process generates a new product (X^-/X^{-2}) that does not appear in the first scanning and increases for the subsequent scanning. However, if the X^{-3} or X^{-4} are unstable in the solution, there will not be much X^{-2} left for a return scan. In other words, X^{-2}/X^{-3} & X^{-3}/X^{-4} undergo an irreversible oxidation process or decomposition.

The peak potential (Ep) depends on the scan rate or concentration if the oxidation peak potential shifts to more positive potentials, and the non-scan rate is dependent if the E_p remains relatively constant as the scan rate and concentration increase. The relationship between these two variables can be determined by plotting the log E_p/i_p vs Log_{10}scan rate (see supporting information). The slope of the plot of log E_p vs log_{10}scan rate provides information about the redox process of the electrochemical reaction, including diffusion-controlled process (slope close to 0.5), adsorption-controlled process (slope close to 1.0)

and mixed diffusion-adsorption process (slope between 0.5 and 1.0). The positive slope of log_{10}ip vs scan rate indicates a linear relationship that suggests the reactions process is electrochemically consistent with the Randles-Sevcik equation. The coefficient determination (R^2 value) indicates the correlation between the E_p/i_p and scan rate. The closer to 0.0, the weaker correlation between the values, and the closer to 1.0, the stronger correlation the value is. In the case of piperine, log_{10} of peak potential (E_p) vs $log_{10}$of scan rate (mVs^{-1}) gave y = 0.0539x + 2.7743 and R^2 = 0.9503 shows that the redox process is diffusion-controlled (slope: 0.0539) and log_{10} of peak current (i_p) log_{10} of scan rate (mVs^{-1}) gave y = 0.5111x + 0.8329 and R^2 = 0.9503 meaning the electrochemical process is consistent with the Randles-Sevcik equation.

Having established that piperine is both electrochemically active and has multiple oxidation events, we then employed our established protocols for Shono-type [31-35] and Oxa-Shono-type oxidations.[36] Piperine was reacted under electrochemical conditions and the series of products resulting were analysed by LC-MS (**Scheme 1** and **Figure 2**).

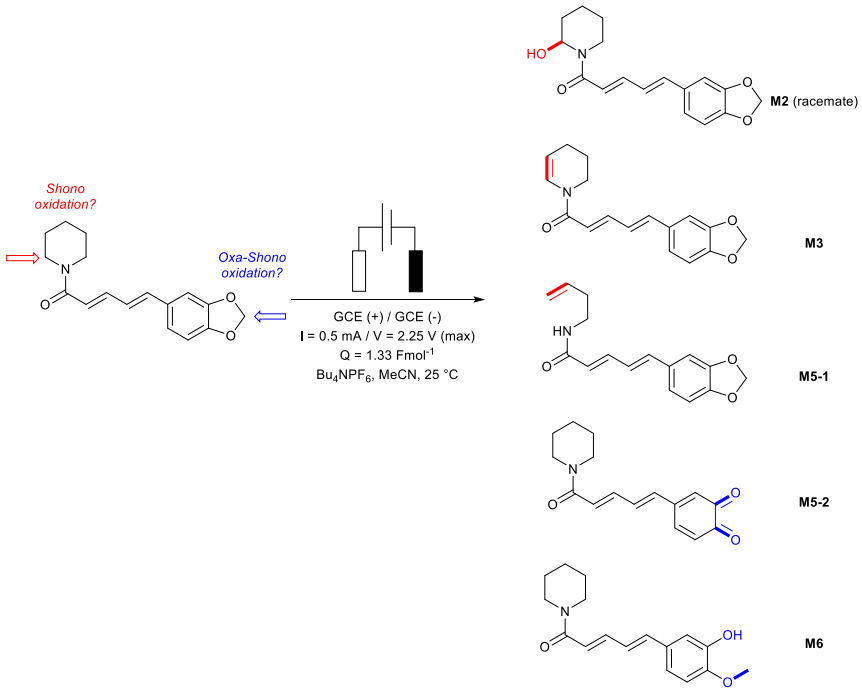

Scheme 1. Electrochemical oxidation of piperine and LC-MS identifiable metabolites. Key: Red indicates Shono-type oxidation reactions, and blue indicates oxa-Shono-type oxidation reactions.

Using MS fragmentation patterns (**Figure 2**), and via comparison with related electrochemical [24] and hepatocyte incubation data, [25] the tentative structures of metabolites 2, 3, 5-1, 5-2, and 6 were determined as shown in **Scheme 1**.

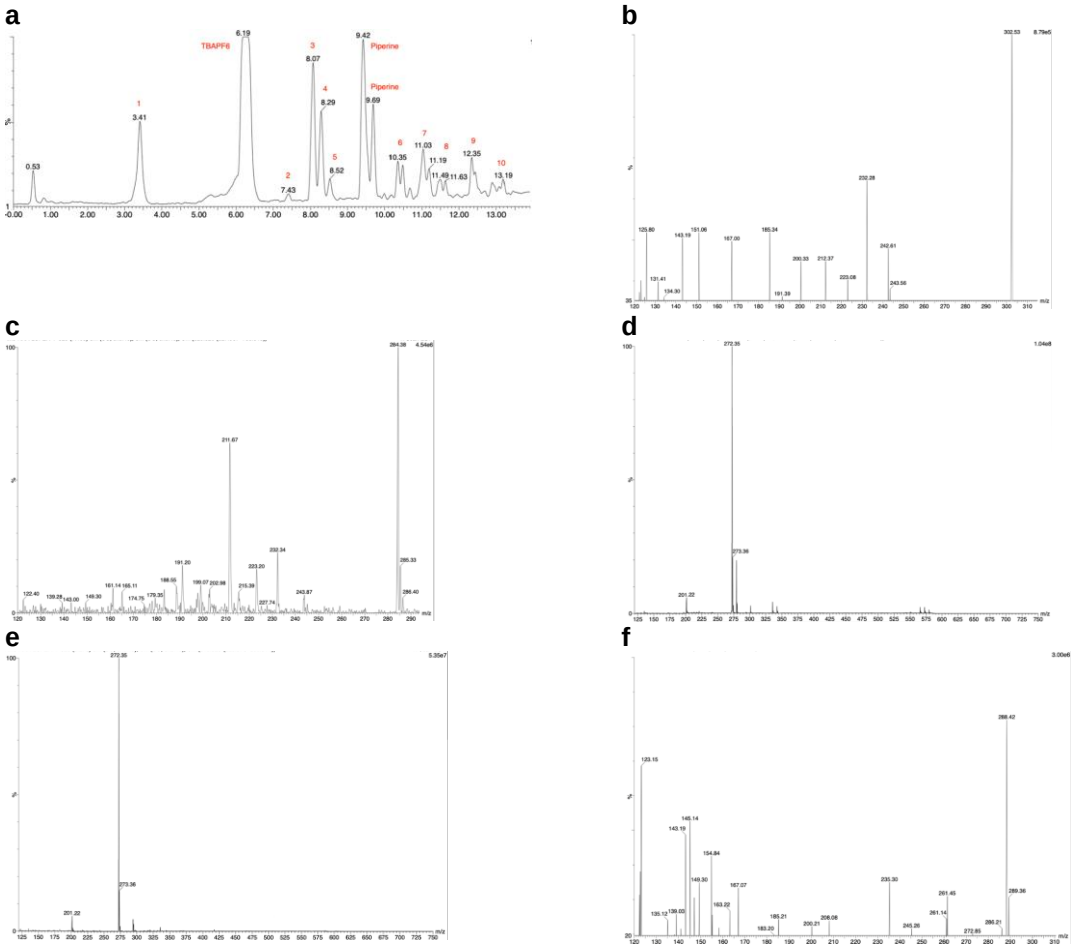

Figure 2. a) LCMS trace for the electrochemical reaction of piperine to a series of metabolites 1-10; **b)** *m/z* of metabolite 2; **c)** *m/z* of metabolite 3; **d)** *m/z* of metabolite 5-1; **e)** *m/z* of metabolite 5-2; and **f)** *m/z* of metabolite 6.

It should be noted that piperine exists a *Z,Z*-conjugated alkene isomer but upon electrochemical reaction *E*,*Z* and/or *Z,E*-isomers form as detected by thin-layer chromatography (TLC) and LC-MS analysis (see supporting information) from a radical isomerism reaction *in situ*. A summary of the overlap between methods (phase II electrochemical and hepatocyte incubation of piperine) and novel metabolites with *this work* are shown in **Table 1**.

Predicted oxidative piperine metabolites	**Electrochemical** Azam et al [24]	**Hepatocytes** Li et al [25]	***This work***
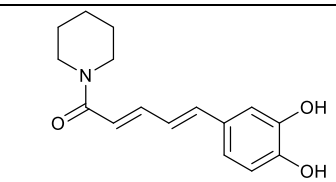	**C12**	**M12**	n.d.
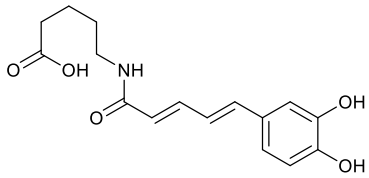	**C4**	n.d.	n.d.
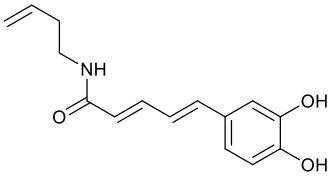	**C8**	**M8**	n.d.
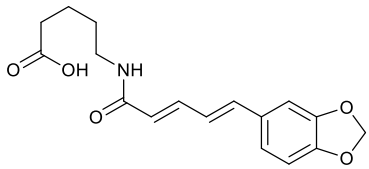	n.d.	**M14**	n.d.
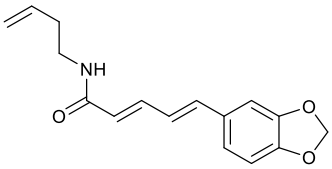	n.d.	**M19**	**M5-1**
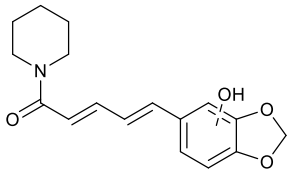	n.d.	**M18**	n.d.
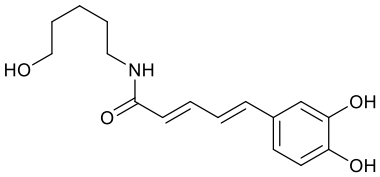	n.d.	**M3**	n.d.
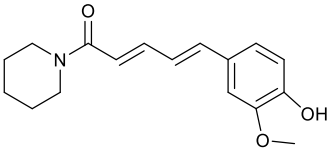	**C17**	n.d.	**M6**
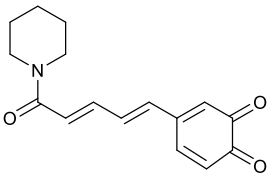	*GSH-adduct Detected via o-quinone*	n.d.	**M5-2**
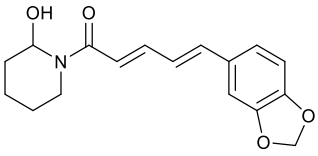	n.d.	n.d.	**M2**

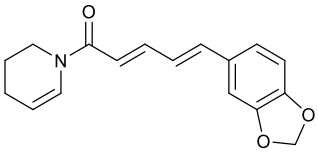	n.d.	n.d.	**M3**

Table 1. Previous detected piperine metabolites from tandem electrochemical-LCMS detection [24], hepatocyte incubation, [25] and *this work*. Codes in columns 2 and 3 e.g. **C#** and **M#** are directly taken from the original literature assignments codes. [24-25]

Furthermore, other unassigned oxidative metabolites were produced in this reaction (see supplementary information). We next considered whether the confirmed or tentatively assigned oxidation metabolites would be possible from a predictive model. To enable this, we employed cytochrome (CYP3A4), a pivotal protein involved in the metabolism of numerous drugs, while piperine acts as an inhibitor of this protein.[22] CYP3A4 inhibition may lead to drug-drug interactions, toxicity, and other adverse effects, but in can also be beneficial and enhance the therapeutic efficiency of co-administered pharmaceuticals that are metabolized by CYP3A4.

The piperine and metabolite structures were optimized by *ab initio* calculation. The calculations were performed using the Gamess2018 quantum mechanics package with Hartree–Fock (HF) formalism and functional density theory (DFT) following the same method of our previous work. [37] The protein structure was obtained from PDB 1TQN and prepared following the same method of our previous work.[38] . Autodock tools 1.5.4 were used to prepare the protein, adding polar hydrogen bonds and Gasteiger charges. The Grid box was built to explore the whole protein (blind docking) with the grid box dimensions as 126×126×126 points with a spacing of 0.458 A˚ and centered at x = -19.213, y =-23.825, and z = -14.03. The protein binding sites were investigated with autodock4.2 using the Lamarckian Genetic Algorithm (LGA) in a total of 100 different conformations. The final poses were selected among the most negative energies.The affinity energy function obtained from our docking of piperine (-8.73 kcal/mol) is very close to the that reported in the literature (-8.55 kcal/mol), which gives us added confidence of the predicted pose of piperine within the active pocket of CYP3A4 (**Figure 2** and **3**).[39]

The *inter*molecular distances between the clustered (see SI) low-energy binding pose of piperine and the *N* and *Fe* atoms of the heme group in CYP3A4 (distances are reported in Å in **Figure 2**). This model is indicative that the benzo[*d*][1,3]dioxole motif is more likely to engage with the heme group and undergo an oxidation event in the body. For instance, metabolites e.g **M8, M12, M18, M3** as detected in a hepatocyte incubation [25] which evaluates both phase I (oxidative) and phase II (conjugation) events. **M5-2** and **M6** from *our work* demonstrates an oxidative event in this fragment of piperine.

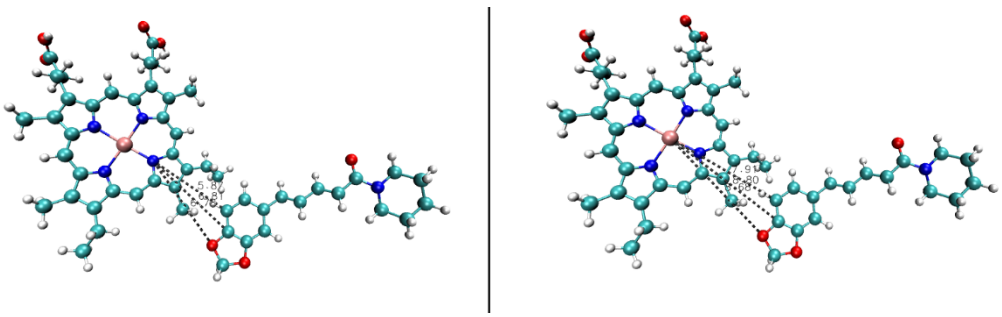

Figure 2. Docking of piperine into the active site of CYP3A4 and resulting in close proximity of piperine to **(a)** the closest heterocycle within porphyorin and **(b)** the closest interaction to the Fe atom. Both depictions, indicate the benzo[*d*][1,3]dioxole motif of piperine as a predicted site for phase I oxidative metabolism in the body.

We next considered whether the metabolites identified from our electrochemical screen (**Scheme 1**) would be feasible to exist in the CYP active pocket, post metabolic oxidation. To achieve this we explored the clustered binding patterns of our piperine metabolites compare to piperine itself within the cytochrome (**Figure 3**). The findings from molecular docking, reveal that metabolites **M2** and **M3** dock precisely in the same region as piperine with an increase in energy score for **M3** and an decrease of energy scores for **M2** (as shown in Table S1). This suggests that upon metabolism, the **M2** metabolite exhibit diminished affinity for the protein.

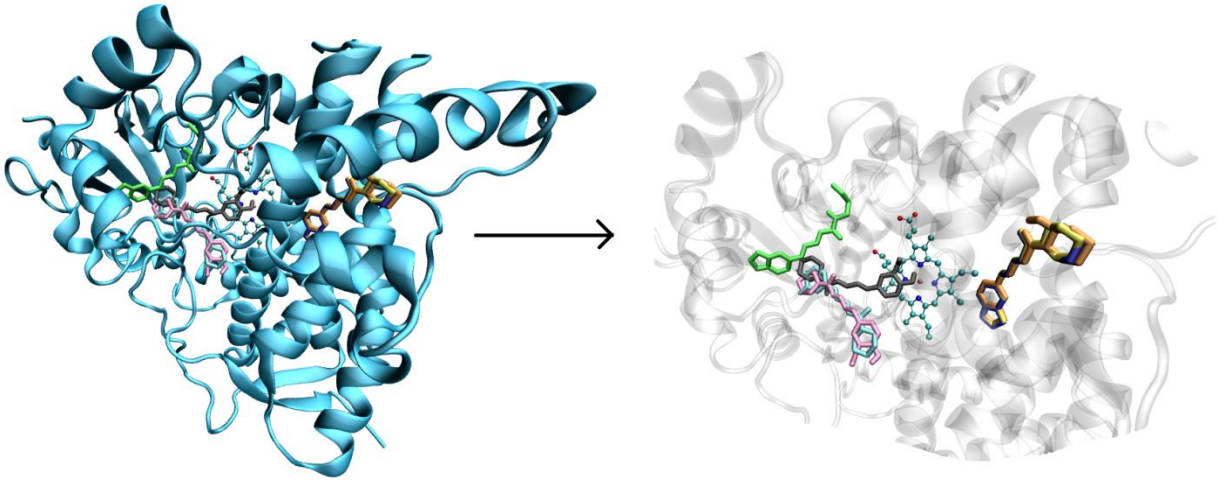

Figure 3. Left- General view of docked molecules into CYP3A4 (**piperine** in blue, **M2** in orange, **M3** in yellow, **M5-1** in green, **M5-2** in cyan, and **M6** in black) . Right – Zoomed-in region. The protein is new cartoon outfit, the molecules in licorice and the heme group in CPK.

One of the highly specific interactions observed is the π-π followed by π-cation interaction, owing to its high level of molecular organization. These interactions are recognized as highly specific molecular recognition interactions in protein-ligand complex, often considered as complex identity interactions. [38, 40-42] Analyzing the results of molecular docking (**Figure 4**), both metabolites **M2** and **M3** exhibit π-π interactions with the heme group of the protein. It is interesting note that **M3** presented an increasing of binding affinity compared to piperine while M2 presented a reduced affinity for the protein compared to piperine. These results strongly suggest that these piperine derivatives might act as protein inhibitors post-metabolism, unless the decreased affinity caused **M2** to vacate the binding site because of competition with other biological molecules. Moreover, Besides π-π interaction, the amino acids performed non specific interactions with piperine, **M2** and **M3** with no hydrogen bonds presented.

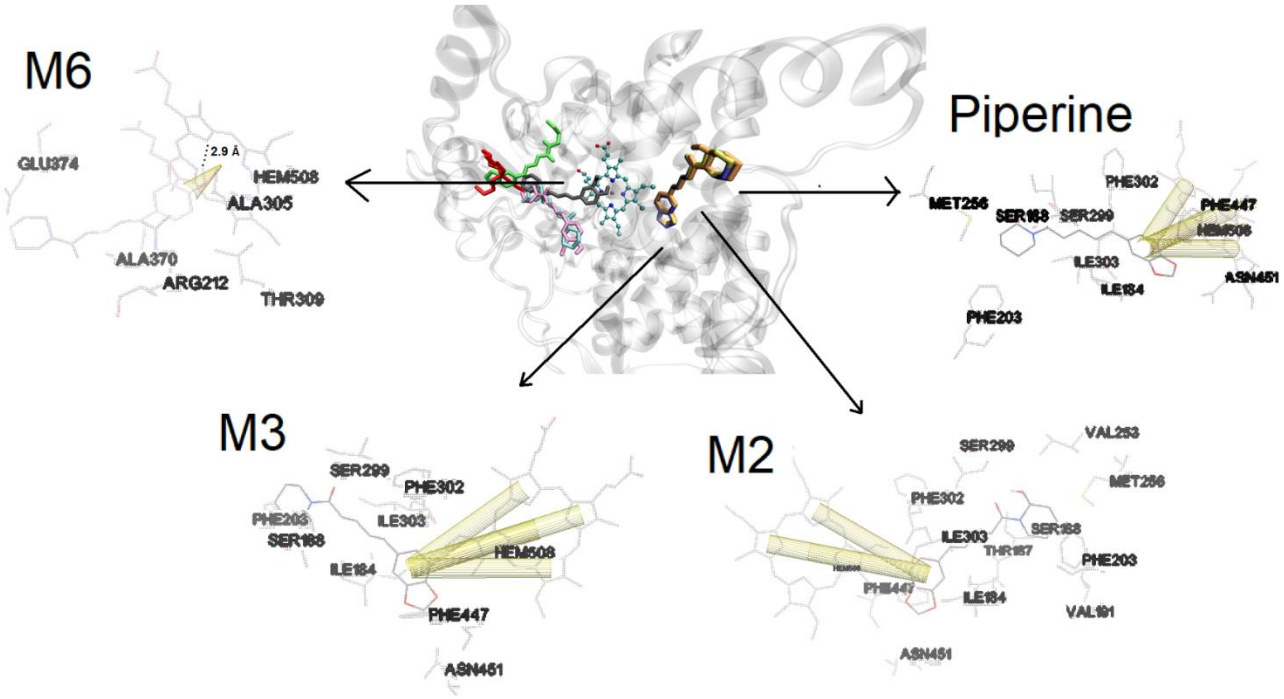

Figure 4. The visualization of the four docking poses (piperine, **M2**, **M3** and **M6**) highlighting the π-π, cation-π and hydrogen bond interactions.

Despite **M6** not binding directly at the piperine site, it still engages in a π-cation interaction with the iron of the heme group and forms a hydrogen bond between the hydroxyl group of **M6** and the heme group (2.9 Å). While **M6** binds to the heme group, it's noteworthy that the π-cation interaction is less specific than π-π interactions, and the metabolite does not bind to the piperine interaction site. This suggests that this metabolite may not have the potential to inhibit the protein. Metabolites **M5-1** and **M5-2** do not interact with the heme group in the two lowest energy poses. The only specific interaction observed is a hydrogen bond formed by metabolite **M5-2** with R212 (2.82 Å), the others interactions are non-specific. Besides that these three metabolites presented lower affinity to protein compared to piperine. This suggest that upon metabolism, the metabolites might leave the protein when in contact with others biological components.

Conclusions

In summary, we have disclosed a direct electrochemical analysis and reaction of piperine and identified a series of chemically plausible metabolites. Furthermore, predictive modelling of piperine identified the most likely region of the molecule to undergo oxidation in the body. Analysis of the piperine metabolites binding pose within the active *heme* pocket of CYP3A4 revealed potential molecules that may lead to the inhibitive activity of piperine reported in the literature. Taken together, we have shown an approach that integrates computational docking, electrochemical reaction, and analytical techniques to predict the likelihood of metabolites in a challenging example. The CP-EDM technique may find use in a range of drug discovery endeavours to expedite the prediction and analytical aspects of drug metabolism.

Acknowledgements

The authors gratefully acknowledge the PhD scholarship of The Center for Education Funding Services (BPI); Ministry of Education, Culture, Research, and Technology; and the Indonesia Endowment Fund for Education (LPDP), Ministry of Finance, The Republic of Indonesia.

References

[1] S. Schadt, B. Bister, S.K. Chowdhury, C. Funk, C.E.C.A. Hop, W.G. Humphreys, et al A Decade in the MIST: Learnings from Investigations of Drug Metabolites in Drug Development under the "Metabolites in Safety Testing" Regulatory Guidance. Drug Metabolism and Disposition 46(6) (June 2018) 865-878; https://doi.org/10.1124/dmd.117.079848

[2] N. Nikzad, M. Rafiee, Electrochemical study of drug metabolism. Current Opinion in Electrochemistry, 44 (2024) 101446, https://doi.org/10.1016/j.coelec.2024.101446.

[3] K.G. Madsen, G.Grönberg, C.Skonberg, U. Jurva, S.H. Hansen, J.Olsen, Electrochemical Oxidation of Troglitazone: Identification and Characterization of the Major Reactive Metabolite in Liver Microsomes. Chemical Research in Toxicology 21(10) (2008) DOI: 10.1021/tx8002214

[4] R. Asra, A.M. Jones, Green electrosynthesis of drug metabolites. Toxicol. Res. 12(2) (2023) 150-177 https://academic.oup.com/toxres/article/12/2/150/7071047

[5] A. Kuzikov, R.Masamrekh, T.Filippova, V.Shumyantseva, Electrochemical Analysis of Metabolites as a Method for Cytochromes P450 Activity Determination. *Biomedical Chemistry: Research and Methods*, *5*(4) (2022) e00176 https://doi.org/10.18097/BMCRM00176

[6] M. H. Rahman, M.K. Bal, A.M. Jones, Metabolism Inspired Electrosynthesis, ChemElectroChem, 6 (2019) 4093-4104, https://chemistry-europe.onlinelibrary.wiley.com/doi/abs/10.1002/celc.201900117

[7] U.Jurva, L. Weidolf, Electrochemical generation of drug metabolites with applications in drug discovery and development, Trends in Analytical Chemistry, 70 (2015) 92–99

[8] K.G. Madsen, J. Olsen, C. Skonberg, S.H. Hansen, U. Jurva, Development and Evaluation of an Electrochemical Method for Studying Reactive Phase-I Metabolites: Correlation to *in Vitro* Drug Metabolism *Chem. Res. Toxicol.* 20 (2007) 821-831

[9] S. Khera, N. Hu, Generation of statin drug metabolites through electrochemical and enzymatic oxidations, Anal Bioanal Chem 405 (2013) 6009–6018

[10] H. Yao, E.C. Sherer, M. Lu, J. Small, G.E. Martin, Y.-h. Lam, et al, One-Step Regio- and Stereoselective Electrochemical Synthesis of Orexin Receptor Antagonist Oxidative Metabolites, *J. Org. Chem.* 87 (2022) 15011−15021

[11] C. Walgama, R. Nerimetla, N. F. Materer, D. Schildkraut, J.F. Elman, S. Krishnan, A Simple Construction of Electrochemical Liver Microsomal Bioreactor for Rapid Drug Metabolism and Inhibition Assays Anal. Chem. 87 (2015) 4712−4718 DOI: 10.1021/ac5044362

[12] A. Potęga, D. Garwolińska, A.M. Nowicka, M. Fau, A. Kot-Wasik, Z. Mazerska, Phase I and phase II metabolism simulation of antitumoractive 2-hydroxyacridinone with electrochemistry coupled on-line with mass spectrometry, Xenobiotica, 49(8) (2019) 922-934, DOI: 10.1080/00498254.2018.1524946

[13] A. Gutmann, L.J. Wesenberg, N. Peez, S.R. Waldvogel, T. Hoffmann, Charged Tags for the Identification of Oxidative Drug Metabolites Based on Electrochemistry and Mass Spectrometry *ChemistryOpen* 9 (2020) 568–572, doi.org/10.1002/open.202000084

[14] R. Stalder, G. P. Roth, Preparative Microfluidic Electrosynthesis of Drug Metabolites, ACS Med. Chem. Lett. 4 (2013) 1119−1123, dx.doi.org/10.1021/ml400316p

[15] Z.Zhang, W. Tang, Drug metabolism in drug discovery and development Acta PharmaceuticaSinicaB 8(5) (2018) 721–732, https://doi.org/10.1016/j.apsb.2018.04.003

[16] Y.Feng, C.Gong, J.Zhu, G.Liu, Y.Tang, W.Li, Prediction of Sites of Metabolism of CYP3A4 Substrates Utilizing Docking-Derived Geometric Features. Journal of Chemical Information and Modeling 63(13) (2023) 4158-4169 DOI: 10.1021/acs.jcim.3c00549

[17] D.K. Lokwani, A.P. Sarkate, K.S.Karnik, A.P.G. Nikalje, J.A. Seijas, Structure-Based Site of Metabolism (SOM) Prediction of Ligand for CYP3A4 Enzyme: Comparison of Glide XP and Induced Fit Docking (IFD). Molecules 25(7) (Apr 2020) 1622. doi: 10.3390/molecules25071622

[18] P.C. Nair, R.A. McKinnon,J.O. Miners, CYP3A4-Mediated SOM Prediction of Protein Kinase Inhibitors. Drug Metabolism and Disposition 47(6) (June 2019), 616-631, https://doi.org/10.1124/dmd.118.085167

[19] G. Zazeri, A.P.R. Povinelli, C.S. Le Duff, B. Tang, M.L. Cornelio, A.M. Jones, Synthesis and Spectroscopic Analysis of Piperine and Piperlongumine-Inspired Natural Product Scaffolds and their Molecular Docking with IL-1β and NF-κB proteins, Molecules 25 (2020) 2841, https://www.mdpi.com/1420-3049/25/12/2841

[20] A.P.R. Povinelli, G. Zazeri, A.M. Jones, M.L. Cornélio, A computational-experimental investigation of the molecular mechanism of Interleukin-6 – piperine interaction, Int. J. Mol. Sci. 23(14) (2022) 7994, https://doi.org/10.3390/ijms23147994

[21] B.R. Pradeepa, T.M. Vijayakumar, K. Manikandan, A.K. Kammala, Cytochrome P450-mediated alterations in clinical pharmacokinetic parameters of conventional drugs coadministered with piperine: a systematic review and meta-analysis. J. Herb. Med. 41 (2023) 100713 https://doi.org/10.1016/j.hermed.2023.100713.

[22] R.K. Bhardwaj, H. Glaeser, L. Becquemont, U. Klotz, S.K. Gupta, M.F. Fromm, Piperine, a major constituent of black pepper, inhibits human P-glycoprotein and CYP3A4. J. Pharmacol. Exp. Ther. 302 (2) (2002) 645-50, doi: 10.1124/jpet.102.034728.

[23] https://biotransformer.ca/new provided no predicted metabolic site on piperine.

[24] S. Azam, J.-Y. Park, I.-S. Kim, D.-K. Choi, Piperine and Its Metabolite's Pharmacology in Neurodegenerative and Neurological Diseases. Biomedicines, 10 (2022)154, https://doi.org/10.3390/biomedicines10010154

[25] Y. Li, M. Li, Z. Wang, M. Wen, J. Tang, Identification of the metabolites of piperine via hepatocyte incubation and liquid chromatography combined with diode-array detection and high-resolution mass spectrometry, *Rapid Commun Mass Spectrom*. 34 (2020) e8947,https://doi.org/10.1002/rcm.8947

[26] P. Praneetha, A. Balhara, M.K. Ladumor, D.K. Singh, A. Patil, J. Preethi, et al Characterization of stable and reactive metabolites of piperine formed on incubation with human liver microsomes. J Mass Spectrom. 54(9) (Sep 2019) 738-749, doi: 10.1002/jms.4424

[27] Z. Shang, W. Cai, Y. Cao, F. Wang, Z. Wang, J. Lu, J. Zhang, An integrated strategy for rapid discovery and identification of the sequential piperine metabolites in rats using ultra high-performance liquid chromatography/high resolution mass spectrometery, Journal of Pharmaceutical and Biomedical Analysis, 146 (2017) 387-401, https://doi.org/10.1016/j.jpba.2017.09.012

[28] O. E. Carp, A. Moraru, M. Pinteala, A. Arvinte, Electrochemical behaviour of piperine. Comparison with control antioxidants, Food Chemistry, 339 (2021) 128110, https://doi.org/10.1016/j.foodchem.2020.128110

[29] H. Fuchigami, M.K. Bal, D.A.C. Brownson, C.E. Banks, A.M. Jones, Voltammetric behaviour of drug molecules as a predictor of metabolic liabilities, Scientia Pharmaceutica, 88 (2020) 46, https://www.mdpi.com/2218-0532/88/4/46

[30] A.A.A. Aljabali, J.E. Barclay, J.N. Butt, G.P. Lomonssoff, D.J. Evans, Redox-active ferrocene-modified *Cowpea mosaic virus*nanoparticles, *Dalton Trans.* 2010 (39) 7569-7574, https://doi.org/10.1039/C0DT00495B

[31] A.M. Jones, Dialling-in New Reactivity into the Shono-type anodic oxidation reaction, The Chemical Record, 21 (2021) 2120, https://onlinelibrary.wiley.com/doi/abs/10.1002/tcr.202000116

[32] A. Wetzel, A.M. Jones, Electrically-driven N(sp2)-C(sp2/3) bond cleavage of sulfonamides, *ACS Sustain. Chem. Eng.* 8 (2020) 3487-3493, https://pubs.acs.org/doi/full/10.1021/acssuschemeng.0c00387

[33] M.K. Bal, C.E. Banks, A.M. Jones, Metabolism mimicry: An electrosynthetic method for the selective deethylation of tertiary benzamides, ChemElectroChem, 6 (2019) 4284-4291, https://chemistry-europe.onlinelibrary.wiley.com/doi/abs/10.1002/celc.201900028

[34] A.M. Jones, C.E. Banks, The Shono-type electroorganic oxidation of unfunctionalised amides. Carbon-carbon bond formation via electrogenerated N-acyliminium ions, Beilstein J. Org. Chem. 10 (2014) 3056–3072, https://www.beilstein-journals.org/bjoc/articles/10/323

[35] P. Alfonso-Súarez, A.V. Kolliopoulos, J.P. Smith, C.E. Banks, A.M. Jones, An Experimentalists Guide to Electrosynthesis: The Shono Oxidation, *Tetrahedron Lett.* 56 (2015) 6863-6867. https://www.sciencedirect.com/science/article/abs/pii/S0040403915302872

[36] M.R. Barone, A.M. Jones, Selective C-H Bond Electro-oxidation of Benzylic Acetates and Alcohols to Benzaldehydes. Org. Biomol. Chem. 15 (2017) 10010-10015. https://pubs.rsc.org/en/content/articlelanding/2017/ob/c7ob02300f

[37] Zazeri, G.; Povinelli, A.P.R.; Lima, M.d.F.; Cornélio, M.L. Experimental Approaches and Computational Modeling of Rat Serum Albumin and Its Interaction with Piperine. *Int. J. Mol. Sci.* **2019**, *20*, 2856. https://doi.org/10.3390/ijms20122856

[38] G. Zazeri, A.P.R. Povinelli, N.M. Pavan, D.R. de Carvalho, C.L. Cardoso, V. Farias Ximenes, Experimental studies and computational modeling on cytochrome c reduction by quercetin: The role of oxidability and binding affinity, Journal of Molecular Structure, 1244 (2021) 130995, https://doi.org/10.1016/j.molstruc.2021.130995

[39] B.R. Pradeepa, T.M. Vijayakumar, L.S. Dhivya,K. Manikandan, *In-silico* comparison of cytochrome P450 inhibitory and dopaminergic activity of Piperine, Curcumin and Capsaicin, Natural Product Research, 37(17) (2023) 2888-2893, DOI: 10.1080/14786419.2022.2134862

[40] T. Damghani, T. Sedghamiz, S. Sharifi, S. Pirhadi, Critical c-Met-inhibitor interactions resolved from molecular dynamics simulations of different c-Met complexes, Journal of Molecular Structure, 1203 (2020) 127456, https://doi.org/10.1016/j.molstruc.2019.127456

[41] N. Sharma, O. Prosser, P. Kumar, A. Tuplin, R. Giri, Small molecule inhibitors possibly targeting the rearrangement of Zika virus envelope protein, Antiviral Research, 182 (2020) 104876, https://doi.org/10.1016/j.antiviral.2020.104876

[42] O. Iwaloye, O. Elekofehinti, A.I. Momoh, et al. In silico molecular studies of natural compounds as possible anti-Alzheimer's agents: ligand-based design. Netw Model Anal Health Inform Bioinforma 9(54) (2020), https://doi.org/10.1007/s13721-020-00262-7